Comparative Evaluation of Three-Phase High-Power-Factor AC–DC Converter Concepts for Application in Future More Electric Aircraft

Guanghai Gong, *Student Member, IEEE*, Marcelo Lobo Heldwein, *Student Member, IEEE*, Uwe Drofenik, *Member, IEEE*, Johann Miniböck, Kazuaki Mino, *Student Member, IEEE*, and Johann W. Kolar, *Senior Member, IEEE*

***Abstract*—A passive 12-pulse rectifier system, a two-level, and a three-level active three-phase pulsewidth-modulation (PWM) rectifier system are analyzed for supplying the dc-voltage link of a 5-kW variable-speed hydraulic pump drive of an electro-hydrostatic actuator to be employed in future More Electric Aircraft. Weight, volume, and efficiency of the concepts are compared for an input phase voltage range of 98–132 V and an input frequency range of 400–800 Hz. The 12-pulse system shows advantages concerning volume, efficiency, and complexity but is characterized by a high system weight. Accordingly, the three-level PWM rectifier is identified as the most advantageous solution. Finally, a novel extension of the 12-pulse rectifier system by turn-off power semiconductors is proposed which allows a control of the output voltage and, therefore, eliminates the dependency on the mains and load condition which constitutes a main drawback of the passive concept.**

***Index Terms*—More Electric Aircraft, pulsewidth-modulation (PWM) rectifier system, 12-pulse rectifier system.**

I. Introduction

LARGE transport category airplanes are currently equipped with three independent hydraulic systems and two independent electrical systems [1]. On future More Electric Aircraft the conventional fly-by-wire hydraulic flight control surface (rudder, aileron, spoiler, etc.) actuation which is supplied from the centralized hydraulic generation and distribution system will be associated with electrically powered electrohydrostatic actuators (EHAs). This will allow for the elimination of one hydraulic system without impairing safety objectives, since one hydraulic supply is replaced by two electrical systems and/or the power source redundancy is increased. Further advantages are higher flexibility in routing and weight and cost savings due to the reduction of the total number of hydraulic generation and distribution components as well as higher efficiency.

The hydraulic power of the EHAs is generated locally by dedicated hydraulic pumps which are driven by variable-speed electric motors being fed by an inverter from a voltage dc link ([2, Fig. 2]). In order to prevent a distortion of the supply voltage and/or interference with sensitive avionics equipment, rectifier concepts with low effects on the mains have to be employed. There, (currently) only unidirectional power conversion is required; energy which is fed from the loaded surface back into the DC link is dissipated in a resistive dump circuit ([3, Fig. 3]).

Rectifier systems with high input current quality basically can be realized as passive multipulse rectifiers or as high-switching-frequency pulsewidth-modulation (PWM) rectifier systems which allow an active control of the shape and phase displacement of the input current and of the output voltage [4]. In order to provide a basis for a decision, both concepts must be compared concerning volume, weight, efficiency, complexity/reliability, and realization costs.

The topic of this paper is a comparative evaluation of a passive autotransformer-based 12-pulse rectifier with capacitive smoothing [see Fig. 1(a)] [5] and of an active three-level boost-type PWM rectifier system [see Fig. 1(b)] [6]. Furthermore, a conventional two-level PWM rectifier concept as known from industrial automation systems is considered for reference purposes [see Fig. 1(c)]. There, the system operating parameters are defined as

$$U_{N,\mathrm{rms}} = 115\ \mathrm{V} \pm 15\% \approx 98\text{–}132\ \mathrm{V}$$
$$f_N = 400\text{–}800\ \mathrm{Hz}$$
$$P_O = 5\ \mathrm{kW}$$

($U_{N,\mathrm{rms}}$ denotes the rms value of the mains phase voltage, f_N is the mains frequency, and P_O is the output power) like those typically given for aileron actuation systems. An actuation system is characterized by a high peak-to-continuous power rating, i.e., short periods (typically, 1–30 s) of high power demand when the control surface is accelerated and moved at high speed against load, and longer periods where the surface is held in a defined position ([2, Fig. 3] or [3, Fig. 6]). In the case at hand P_O represents an average power level which is considered as continuous output power demand in a rough first approximation.

In a similar way the specified input voltage range $U_{N,\mathrm{rms}} =$ 98–132 V (115 V$\pm$15%) considers long-duration transients in normal operation down to a fraction of an actuation interval (see [3, Fig. 2]).

Currently, for the generation of constant-frequency (400 Hz) ac voltages from variable-frequency engine shafts, complex hydraulic systems are employed which will be replaced in the future by less complex lighter variable-speed generators in combination with power electronics (see [7, p. 249]). Accordingly,

Manuscript received December 12, 2003; revised January 22, 2004. Abstract published on the Internet March 14, 2005. This paper was presented at the 19th IEEE Applied Power Electronics Conference and Exposition, Anaheim, CA, February 22–26, 2004.

The authors are with the Power Electronic Systems Laboratory, Swiss Federal Institute of Technology (ETH) Zurich, CH-8092 Zurich, Switzerland (e-mail: kolar@lem.ee.ethz.ch).

Digital Object Identifier 10.1109/TIE.2005.843957

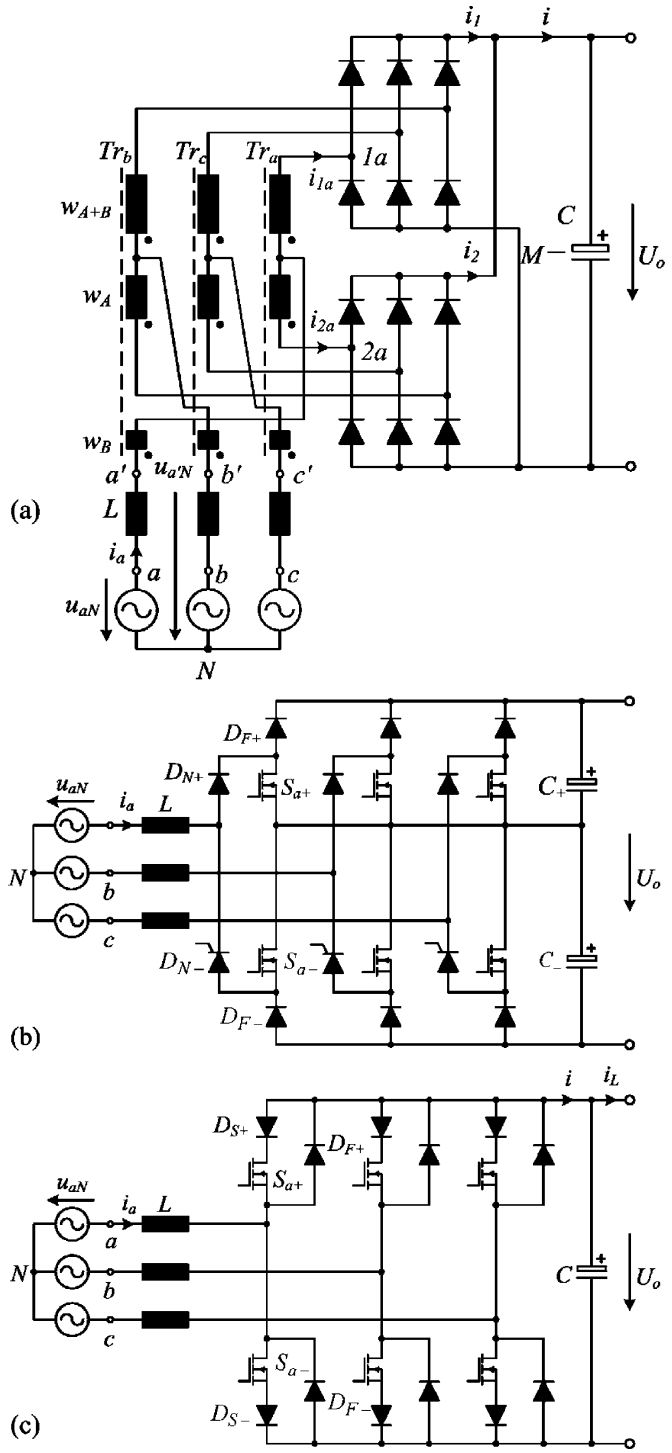

Fig. 1. Three-phase ac/dc converter concepts with low effects on the mains. (a) 12-pulse passive rectifier according to [5]. (b) Unidirectional three-level PWM rectifier according to [6]. (c) Conventional two-level PWM rectifier.

a wide input frequency range of $f_N = 360$–800 Hz (see [8, p. 5]) will be required for future aircraft. As 360 Hz is close to today's nominal frequency $f_N = 400$ Hz, for limiting it to the essentials only, the input frequency range $f_N = 400$–800 Hz is considered in the following.

In Sections II and III, the basic function of the rectifier systems is discussed briefly and the distribution of the losses to the main power components is shown. There, the calculation of the power semiconductor losses refers to on-state characteristics given in the data sheets and to measured switching losses where $T_j = 125$ °C is assumed in general for the junction temperature. For the selection of the power transistors and power diodes, a heat-sink temperature of $T_s = 80$ °C is considered and the dimensioning of the heat sink and the forced-air cooling is based on an ambient temperature of $T_a = 50$ °C. The winding temperature of the inductive components taking influence on the winding losses is estimated as $T_w = 90$ °C. In Section IV, a comparative evaluation of the concepts concerning volume, weight, and efficiency is given considering worst case operating points as resulting from the specified input voltage and input frequency range. There, the calculation of the efficiency is based on the sum of the individual loss components of a system as calculated in Sections II or III. This concept has been proven to show a sufficient accurracy of $\pm 0.3\%$ of the efficiency and/or $\pm 10\%$ of the losses with reference to measured values for an efficiency in the range of 97% (see [9, Table 1 and Fig. 9]) as typically also given in the case at hand. In Section V, a novel concept for controlling the output voltage of the 12-pulse rectifier is proposed and experimentally verified. Finally, in Section VI, topics of further research are identified which will include an active buck-type PWM rectifier system which allows a direct system startup without output voltage precharging and/or the limitation of the input current in case of an output short circuit.

II. 12-Pulse Autotransformer Rectifier System

In order to eliminate low-frequency input current harmonics, six-pulse diode bridge rectifier systems could be combined into multipulse systems using phase-shifting isolation or autotransformers. In the case at hand, the 12-pulse rectifier concept shown in Fig. 1(a) with impressed output voltage, mains side interphase transformer [5], and input inductors is considered which directly provides the dc-link voltage of a PWM inverter connected in series. Alternatively, a rectifier system with dc-side interphase transformer [6] could be employed. Both concepts are characterized by an about equal total rated power of the magnetic components, i.e., of the autotransformer and the ac or dc side inductors of $\approx$20% of the dc output power. However, for the system according to [6] higher amplitudes of the input current harmonics would occur ([5, Fig. 4] and [10, Fig. 4(b)]) and the blocking voltage stress on the rectifier diodes would not be defined directly by the output voltage.

The time behavior of characteristic quantities of the 12-pulse rectifier system is depicted in Fig. 2. The autotransformer (interphase transformer) provides a symmetric splitting of the largely sinusoidal mains current into two partial current systems i_{1a}, i_{1b}, i_{1c} and i_{2a}, i_{2b}, i_{2c} (see i_a and i_{1a}, i_{2a} in Fig. 2) with a phase displacement of $\pm 15°$. Due to the continuous shape of the phase currents i_{1i} and i_{2i}, $i = a, b, c$, the rectifier bridge input voltages will show a square-wave shape with reference to the center point M of the output voltage U_O where the voltages of corresponding phases, e.g., u_{1aM} and u_{2aM}, will exhibit a phase difference of 30° in correspondence to the phase displacement of the related phase currents i_{1a} und i_{2a}. After subtraction of the zero-sequence components $u_{1,0} = 1/3 \cdot \Sigma u_{1iM}$ and $u_{2,0} = 1/3 \cdot \Sigma u_{2iM}$ $(i = a, b, c)$ contained in the voltage systems $u_{1aM}, u_{1bM}, u_{1cM}$ and $u_{2aM}, u_{2bM}, u_{2cM}$ the six-pulse voltage systems $u'_{1i} = u_{1iM} - u_{1,0}$ and $u'_{2i} = u_{2iM} - u_{2,0}$ are

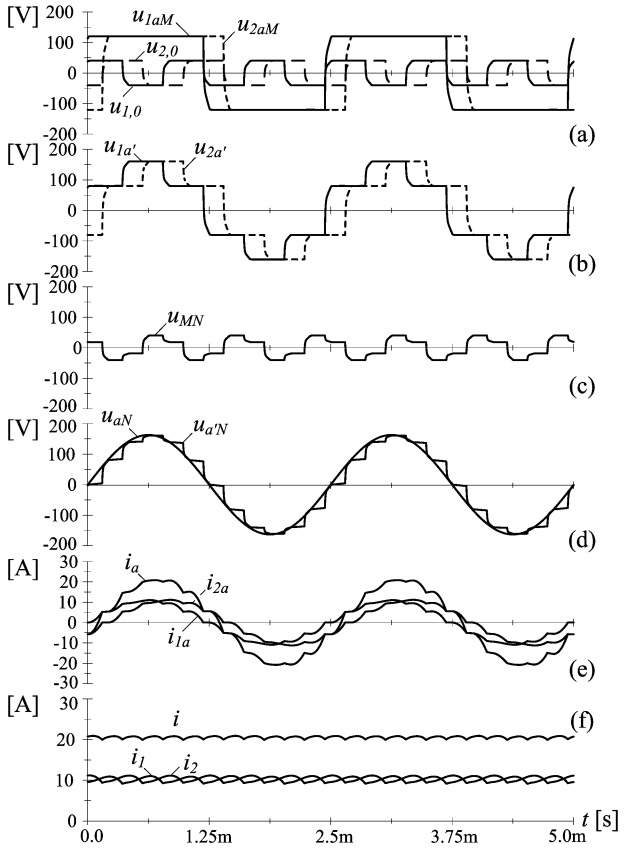

Fig. 2. Operating behavior of the passive 12-pulse rectifier system shown in Fig. 1(a). (a) Input phase voltage of corresponding diode rectifier bridge legs with reference to the dc output voltage center point M and zero-sequence components $u_{1,0}$, $u_{2,0}$ contained in the output phase voltages of the diode rectifier bridges. (b) Zero-sequence free components u'_{1a}, u'_{2a} of the phase voltages shown in (a). (c) Common-mode component u_{MN} of the output voltage. (d) Mains phase voltage u_{aN} and corresponding input phase voltage $u_{a'N}$ of the line interphase transformer. (e) Mains phase current i_a and input currents i_{1a}, i_{2a} of the corresponding interphase transformer windings. (f) Output currents i_1, i_2 of the rectifier bridges and total dc current i. Simulation parameters: $\hat{U}_N = 115$ V; and $f_N = 400$ Hz; $P_O = 5$ kW. For further parameters see Table I; for each phase ideal magnetic coupling of the windings of the interphase transformer has been assumed.

remaining at the autotransformer outputs. There, corresponding voltages, i.e., u'_{1i} and u'_{2i} again show a phase displacement of 30° and are combined by the autotransformer into a 12-pulse voltage system occurring at the input terminals a', b', c' (see, e.g., $u_{a'N}$ in Fig. 2).

The difference of the autotransformer input voltage $u_{i'N}$ and the mains voltage u_{iN} occurs across the input inductors L and defines a mains current i_i of largely sinusoidal shape as only harmonics with ordinal numbers $n = 11$, 13, 23,25 are present in $u_{i'N}$.

Due to the low distortion of the mains current the instantaneous system input power is largely constant which results in a largely constant dc output current i. Accordingly, a low current stress on the output capacitor will occur and the output voltage will show a low ripple also for low smoothing capacitance C_O.

According to [5], $w_B/w_A = 0.366$ has to be selected for the autotransformer windings in order to guarantee a balancing of the ampere-turns of the corresponding phase windings and/or to achieve the above-mentioned symmetric current splitting of the

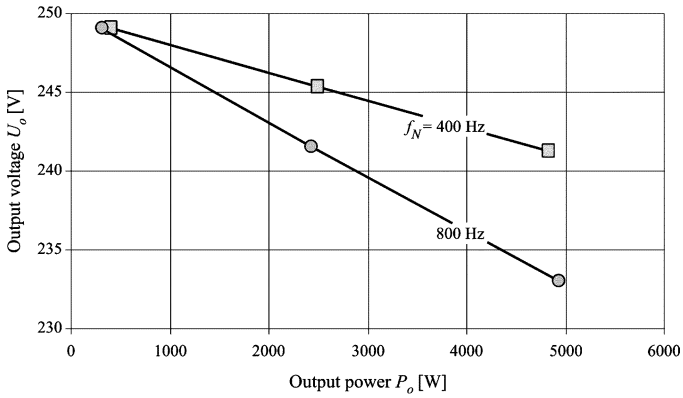

Fig. 3. Dependency of the rectifier output voltage on the output power for $U_{N,\mathrm{rms}} = 115$ V and mains frequencies $f_N = 400$ Hz, 800 Hz as determined by digital simulation. Simulation parameters: see Table I, coupling of the windings of a phase leg of the inpterphase transformer assumed ideal.

mains current and/or 12-pulse combination of the diode bridge input voltages.

The fundamentals of the corresponding phase voltages and currents at the rectifier bridge inputs do not show a phase displacement (see, e.g., u'_{1a} and i_{1a} in Fig. 2). Accordingly, for limiting it to the fundamentals, symmetric three-phase ohmic loads can be assumed at the autotransformer outputs which translates into an ohmic autotransformer fundamental input behavior. Considering the fundamental voltage drop across the input inductors we have, therefore, for the phase displacement of the mains voltage and mains current fundamental

$$\cos\varphi = \sqrt{1 - \left(\frac{\omega L \hat{I}_{N,(1)}}{\hat{U}_N}\right)^2} \tag{1}$$

(see [5, eq.(3.1.1/13)], $\hat{U}_N$ denotes the amplitude of the purely sinusoidal mains voltage, and $\hat{I}_{N,(1)}$ is the amplitude of the mains current fundamental). Neglecting system losses the system output power is then given by

$$P_O = \frac{3}{2}\hat{U}_N \hat{I}_{N,(1)} \cos\varphi = \frac{3}{2}\hat{U}_N \hat{I}_{N,(1)} \sqrt{1 - \left(\frac{\omega L \hat{I}_{N,(1)}}{\hat{U}_N}\right)^2}. \tag{2}$$

In [5], the fundamental of the 12-pulse phase voltages $u_{i'N}$ at the autotransformer input has been shown to be

$$\hat{U}_{U,(1)} = \frac{2}{3} U_O \frac{\sin\frac{\pi}{12}}{\frac{\pi}{12}} \approx 0.66 U_O. \tag{3}$$

For light load (Index 0) only a low fundamental voltage drop across the input inductors occurs and/or $\hat{U}_{U,(1),0} \approx \hat{U}_N$ or $U_{O,0} \approx 1,52\hat{U}_N$ [considering (3)] is valid. Accordingly, we have for the output voltage at larger load (continuous shape of the bridge rectifier input phase currents) under neglection of the conduction voltage drops of the diodes and the parasitic windings resistances and under assumption of an ideal coupling of the autotransformer phase windings

$$U_O \approx U_{O,0} \cos\varphi \approx 1.52 \hat{U}_N \cos\varphi \tag{4}$$

TABLE I
MAIN POWER COMPONENTS EMPLOYED IN THE 12-PULSE AUTOTRANSFORMER RECTIFIER

Part	Quantity	Type	Manufacturer	Typical Data	Package
L	1	Core: S3U 39b / TRAFOPERM N2 0.1mm 31 turns / 0.72 mm air gap	VAC	376 µH / 27.3 A	
$Tr_{a,b,c}$	3	Core: SM55 / TRAFOPERM N2 0.1mm	VAC	w_A/w_B = 34/12	`
C	2	56 µF / 450 V / 105°C / AXF	Rubycon	0.45 A @120 Hz	∅25 x 20 mm
D	12	10ETF04	IR	400 V / 10 A	TO220

(see [5, eq.(3.1.1/12)] and Fig. 6). The actual dependency of the output voltage determined by a digital simulation shown in Fig. 3 reveals that (4) only constitutes a very rough approximation. This is due to the fact that the assumed continuous shape of the bridge rectifier input currents and/or pure staircase shape of the voltages $u_{i'N}$ [see (3)] is only given for high output power and/or close to rated load (see $u_{a'N}$ in Fig. (2c) and [5, Fig. 4]). For low output power the current conduction of the diode bridges is discontinuous and sinusoidal segments of the autotransformer input voltage occur, resulting in $U_O > U_{O,0}$. For no-load operation, the dc output voltage reaches the amplitude of the mains line-to-line voltage $U_{O,\max} = \sqrt{3}\hat{U}_N$ (see Fig. 6). Equation (4), therefore, can only be employed for the calculation of the output voltage resulting for rated load.

The input current harmonics $\hat{I}_{N,(n)}$ are determined by the harmonics of the autotransformer input voltage

$$\hat{U}_{U,(n)} = \frac{1}{n}\hat{U}_{U,(1)} \tag{5}$$

with ordinal numbers $n = 11, 13, 17, 19, \ldots$ and the inductance L connected in series

$$\hat{I}_{N,(n)} = \frac{1}{n^2\omega L}\hat{U}_{U,(1)}. \tag{6}$$

Accordingly, for limiting the low-frequency current harmonics within the entire input voltage and frequency range to given values, e.g.,

$$\begin{aligned}\hat{I}_{N,(11),r} &= 0.1\hat{I}_{N,(1),r}\\ \hat{I}_{N,(13),r} &= 0.08\hat{I}_{N,(1),r}\end{aligned} \tag{7}$$

(for rated power, see [3])

$$L \geq \frac{1}{n^2\omega_{\min}}\frac{\hat{U}_{U,(1),\max}}{\hat{I}_{N,(n)}} \tag{8}$$

has to be ensured. There, $\hat{U}_{U,(1),\max}$ corresponds to the maximum mains voltage and $\omega_{\min}$ is the minimum mains angular frequency.

In the case at hand, we select the minimum value $L = 376\,\mu$H (see Table I) as the actually occurring current harmonics (see Fig. 4) show lower amplitudes than those defined by (6). This is again [as for (4)] caused by the discontinuity of the diode bridge input currents in the vicinity of the zero crossings which results

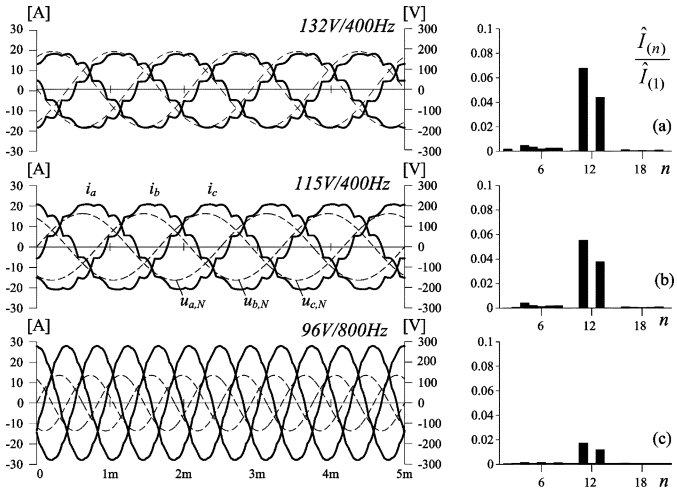

Fig. 4. Time behavior of the mains current and related low-frequency harmonics (normalized to the amplitude $\hat{I}_{N,(1)}$ of the fundamental) for (a) maximum input voltage, $U_{N,\mathrm{rms}} = 132$ V, and minimum input frequency, $f_N = 400$ Hz (worst case concerning the amplitudes of the current harmonics). (b) Rated mains voltage and rated frequency, $U_{N,\mathrm{rms}} = 115$ V, $f_N = 400$ Hz. (c) Minimum input voltage $U_{N,\mathrm{rms}} = 98$ V and maximum frequency $f_N = 800$ Hz.

in an autotransformer input voltage of lower low-frequency harmonic content. An experimental analysis verifying the simulation results shown in Figs. 2 and 4 is given in [11] for a system of 10-kW rated power (see [11, Figs. 2 and 3]) and, therefore, shall be omitted here for the sake of brevity.

As at the outputs $(1a, 1b, 1c)$ and $(2a, 2b, 2c)$ of the autotransformer different zero-sequence voltages $u_{1,0}$ and $u_{2,0}$ [see Fig. 2(a)] are present, a zero-sequence voltage occurs across each set of phase windings. Therefore, the autotransformer has to be realized using individual magnetic cores for the phases or a common five-limb core which allows for accommodating a zero-sequence magnetic flux. The magnetic flux occurring in an individual core is determined by the difference of the phase voltages at the corresponding outputs, e.g., u_{1aM} and u_{2aM}. Concerning further details of the dimensioning of the system we would like to refer to [5] (see [5, Fig. 2]) for the sake of brevity.

In summary, the 12-pulse rectifier is characterized by a total rated power of all magnetic components (autotransformer and input inductors L) of ≈20% of the dc power. The main components to be employed in the power circuit are compiled in Table I, and the losses in the power components are shown in Fig. 5 (concerning the resulting efficiency see Fig. 11).

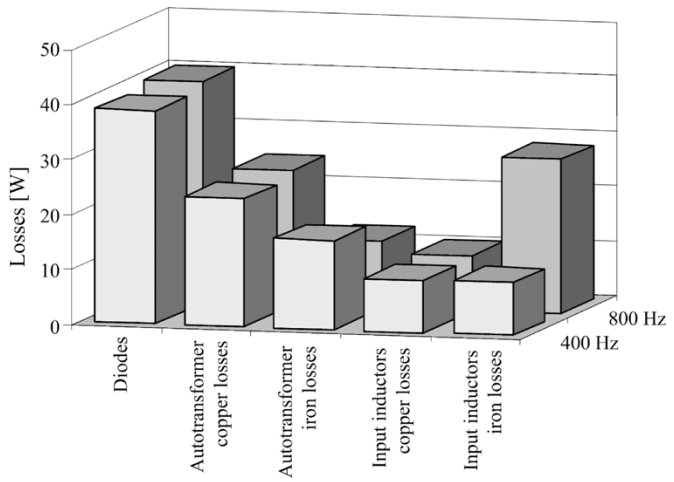

Fig. 5. Distribution of the losses for $U_{N,\mathrm{rms}} = 115$ V and different mains frequencies $f_N = 400$ Hz and 800 Hz. Frequency-dependent losses of the windings of the inductive components due to skin and proximity effect and eddy currents are not considered. Iron losses of the interphase transformer decrease with increasing frequency because of the decreasing amplitude of the magnetic flux density. On the other hand, the iron losses of the input-side inductances increase with increasing frequency as the current is defined for a certain output power and mains voltage amplitude and the hysteresis losses are increasing with increasing frequency.

Compared to active solutions, passive rectifier systems show a relatively high overload capacity of the power components which makes such systems especially interesting for applications requiring high peak-to-continuous power demand. If a largely sinusoidal shape of the mains current should be also given for overload conditions, the magnetic design of the input inductors has to ensure that, up to the maximum output power, no magnetic saturation occurs.

One has to note that according to (1) the mains phase currents and voltages show an increasing phase displacement with increasing output power (with decreasing output resistance and/or increasing amplitude $\hat{I}_{N,(1)}$ of the mains current fundamental). As can be derived from (2) and/or from a phasor diagram, the output power of the system reaches a maximum for $\hat{I}_{N,(1)} = \hat{U}_N/(\sqrt{2}\omega L)$ and/or a phase displacement of $\varphi = 45°$ (load/source matching)

$$P_{O,\max} = \frac{3}{2}\frac{\hat{U}_N^2}{2\omega L} \tag{9}$$

(see Fig. 6). A further decrease of the load resistance results in an increase of the mains current amplitude, but due to the increasing phase displacement, the power delivered to the output decreases further and, therefore, also the output voltage. One has to consider the power limit according to (9) when designing a system with a desired maximum output power. Here, the operation at minimum mains voltage and maximum mains frequency is critical (see Fig. 6). If low amplitudes of the 11th and 13th mains current harmonics are required the input inductors have to show a high inductance L which means that the desired output power could not be available for certain operating conditions.

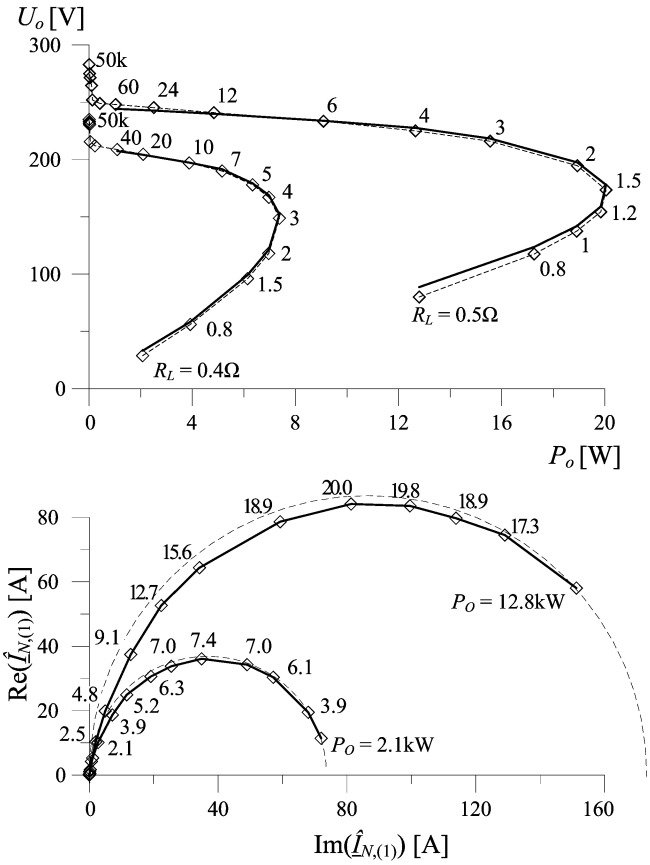

Fig. 6. Simulation (a) of the dependency of the output voltage U_O on the output power P_O (parameter: load resistor) and (b) of the trajectory of the phasor of the mains current (the mains voltage is assumed to be lying in parallel to the vertical real axis; parameter: P_O). Simulation parameters: $U_{N,\mathrm{rms}} = 115$ V@$f_N = 400$ Hz, and $U_{N,\mathrm{rms}} = 98$ V at $f_N = 800$ Hz. For further parameters see Table I. The analytically calculated dependencies of the quantities [see (1)–(4)] are drawn in dashed lines. For small output power the current of the diodes is discontinuous and the output voltage increases to the peak value of the line-to-line mains voltage $U_{O,\max} = \sqrt{6}U_{N,\mathrm{rms}}$ (281.7 V and/or 240 V).

III. Three-Phase PWM Rectifier Systems

A. Unidirectional Three-Level PWM Rectifier

Three-phase PWM rectifier systems allow the formation of pulsewidth-modulated voltages of sinusoidal local average value at the bridge leg inputs. In combination with the mains voltages this results in a sinusoidal mains current and/or no low-frequency harmonics occur. The switching frequency current harmonics can be suppressed by a mains-side filter of relatively small volume.

If no energy feedback into the mains is required the three-level PWM rectifier system given in Fig. 1(b) shows significant advantages compared to a conventional two-level system realization [see Fig. 1(c)]. Besides the potential of the positive and negative dc voltage bus the neutral point potential is also available for voltage formation. The mains phase currents therefore show a lower switching-frequency current ripple and/or input inductors of smaller value and smaller size can be employed. Furthermore, all power semiconductors face only half of the output voltage, resulting in a reduction of the switching losses

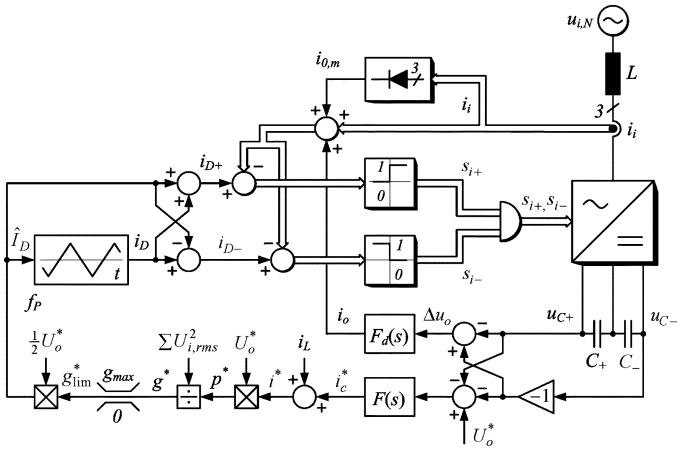

Fig. 7. Cascaded control of a unidirectional three-level PWM rectifier system [see Fig. 1(a)] according to [12]. Signal paths being equal for all phases are combined in double lines.

approximately by a factor of two. Accordingly, this results in an increase of the efficiency of the system, a reduction of the cooling effort, and a further increase of the power density.

The output voltage of the system has to be set higher than the amplitude of the line-to-line mains voltage ($\hat{U}_{N,l-l} \approx 323$ V for $U_{N,\mathrm{rms}} = 132$ V) and is defined in the following as $U_O = 350$ V. The precharging of the output capacitors is performed by precharging resistors which are short circuited by thyristors D_{N-} which perform the rectifier function for regular operation [see Fig. 1(b)]. A pre-charging relay can, therefore, be omitted.

Fig. 7 shows the block diagram of a system control proposed in [12] which guarantees operation of the rectifier also in the case of a loss of one phase. The total output voltage $u_{C+} - u_{C-}$ (u_{C+} and u_{C-} are defined with reference to the output voltage central point M) is compared to the reference voltage U_O^*. Dependent on the control error a reference value of the charging current i_C^* of the output capacitors is formed. Adding the load current (in case of load current precontrol) results in a reference dc current i^* to be fed into the output circuit. Considering the mains voltage condition and a power balance, the reference dc current i^* can be transformed into a reference amplitude of the mains current which is proportional to the amplitude $\hat{I}_D$ of the switching frequency carrier signal i_D of the current control (see Fig. 7). The equal distribution of the total output voltage u_O between the capacitors C_+ and C_- and/or the potential of the output voltage center point M is controlled by an offset i_0 of the three-phase current values, resulting in a center point current. Concerning the detailed function of the control scheme we would like to refer to [12] for the sake of brevity.

The time behavior of input phase currents and of the mains currents resulting after single-stage *LC* filtering is given in Fig. 8 for a switching frequency of $f_P = 50$ kHz ($T_P = 20$ μs). This is a compromise between switching losses, sufficient pulse number within the mains period at maximum mains frequency $f_{N,\max} = 800$ Hz ($T_N = 1250$ μs), and volume of the input side inductors L. The selection of $f_P = 50$ kHz is also with reference to [9] where $f_P = 38$ kHz has proven advantageous for an output voltage of 800 Vdc and/or 600-V power semiconductor technology showing higher switching losses than 300-V power semiconductors employed in the case at hand. In [12, Fig. 1.8] the mains voltage proportional shape of the rectifier input current is also verified for the control concept shown in Fig. 7 and 10-kW rated power, therefore, experimental results shall be omitted here for the sake of brevity.

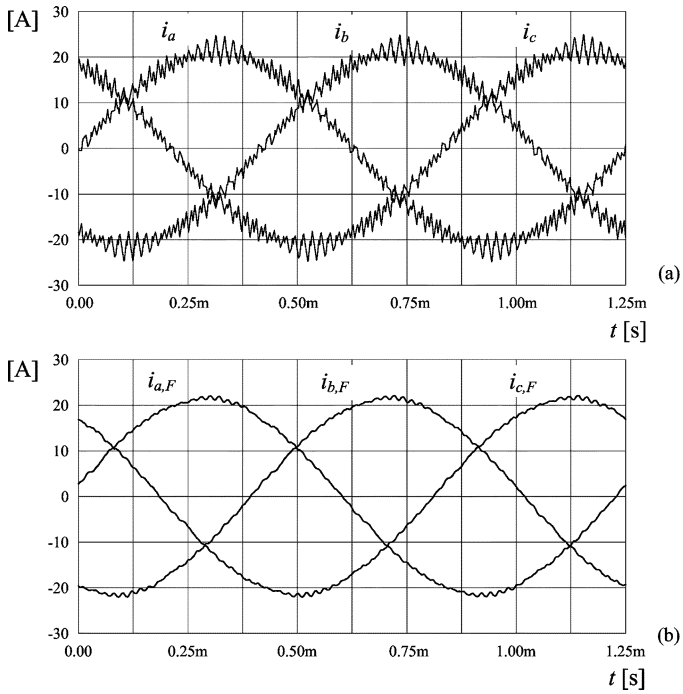

Fig. 8. (a) Simulated time behavior of the rectifier input phase currents i_i, $i = R, S, T$ and (b) of the mains currents $i_{i,F}$ resulting after single-stage *LC* filtering (damping resistor connected in parallel with the filter inductor in order to provide passive filter damping). To fulfill the requirements concerning electromagnetic compatibility (EMC) for a practical realization, generally, a multistage input filter has to be employed. Furthermore, we want to point out that the output voltage of active three-phase PWM rectifier systems shows a common-mode voltage component with switching frequency. Simulation parameters: $U_{N,\mathrm{rms}} = 115$ V; $f_N = 800$ Hz; $U_O = 350$ V; and switching frequency $f_P = 50$ kHz.

The selection of the power components given in Table II can be derived from the analytical expressions of the current stresses of the components given in [13]. The resulting distribution of the system losses at rated power are compared to a conventional PWM converter system [see Fig. 1(c)] in Fig. 9.

B. Two-Level PWM Rectifier

PWM rectifier systems for industrial drives are generally realized as two-level topologies [see Fig. 1(c)] where the pulsewidth-modulated input voltage is formed by switching between positive and negative output voltage bus. This results in a relatively high blocking voltage stress of the power semiconductors defined by the total output voltage that is again chosen as $U_O = 350$ V. Because of the relatively high reverse-recovery time of the internal diodes of the power MOSFETs, one has to provide explicit freewheeling diodes for high switching frequencies [see Fig. 1(c)]. Furthermore, a relay short circuiting the precharging resistors in regular operation has to be employed for a two-level system.

Concerning the output voltage and mains current control and the resulting time behavior of the input and mains currents there are no basic differences between the two-level and the

TABLE II
MAIN POWER COMPONENTS EMPLOYED IN THE 5-kW UNIDIRECTIONAL THREE-LEVEL PWM RECTIFIER SYSTEM

Part	Quantity	Type	Manufacturer	Typical Data	Package
L	3	107µH / 17.8 A_{DC} (33667)	Schott	Helical winding	125 Series
C	10	100µF / 250V / 105°C / YXF	Rubycon	1.2 A / 0.18 Ω	∅18 x 35.5 mm
D_{N-}	3	TYN640 (Thyristor)	ST	600 V / 40 A	TO220
D_{N+}	3	15ETH03	IR	300 V / 15 A / 40 ns	TO220
D_F	6	15ETH03	IR	300 V / 15 A / 40 ns	TO220
S	6	STU26NM50	ST	500 V / 26 A / 0.10 mΩ	TO220

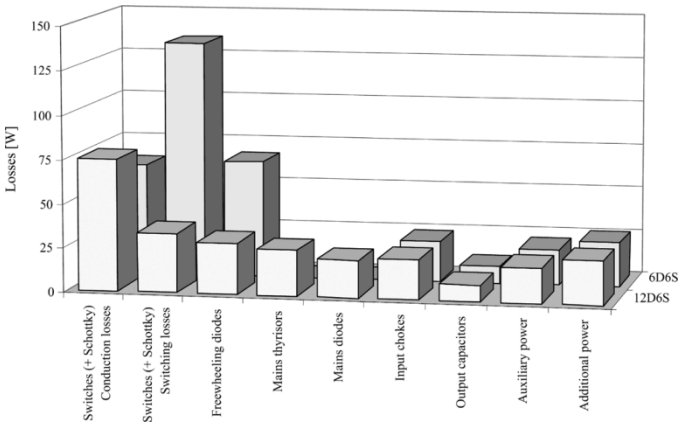

Fig. 9. Distribution of the system losses for the unidirectional three-level PWM rectifier system [comprising 12 diodes and six switches, 12D6S, see Fig. 1(b)] and for the bidirectional two-level PWM rectifier system [comprising six switches and six antiparallel diodes, 6D6S, see Fig. 1(c)]. The considerably higher switching losses of the 6D6S are mainly due to the slower reverse-recovery behavior of the employed 600-V diodes as compared to 300-V diode technology used in the 12D6S. Assumed operating parameters: input voltage $U_{N,\mathrm{rms}} = 115$ V; $U_O = 350$ V; $P_O = 5$ kW; and $f_P = 50$ kHz.

three-level PWM rectifier system discussed in Section III-A, except the higher switching frequency harmonics of the two-level system. We therefore would like to omit a detailed discussion for the sake of brevity.

For the dimensioning of the power components, analytical expressions for the current stresses on the components are given in [14]. The selected components are listed in Table III.

The comparison of the loss distribution of the two-level and the three-level system (see Fig. 9) clearly shows the disadvantages of the conventional realization employing two-level technology. Higher turn-off voltages of the power transistors and a higher reverse-recovery time of the diodes with higher blocking capability result in higher switching losses and, therefore, in a significantly reduced overall system efficiency (see Fig. 11).

IV. COMPARISON OF CONVERTER CONCEPTS

A comparison of the rectifier systems concerning volume (see Fig. 10 and Table IV) identifies a minor advantage of the 12-pulse system even in comparison to the three-level PWM rectifier (denoted as 12D6S in the following). On the other hand, the weight of the 12D6S converter is considerably lower than for the passive 12-pulse system as the heat sink constitutes a considerable share of the total converter volume but shows a low specific weight (see Table V) compared to the magnetic components dominating the 12-pulse system.

The two-level rectifier system (6D6S) exhibits disadvantages concerning the power density due to the high cooling effort resulting from the high switching losses. The overall system weight is about equal to the weight of the 12-pulse rectifier.

Due to the missing switching losses and the low number of power semiconductor forward voltage drops in the main current paths, the efficiency of the 12-pulse system is significantly higher than for the active rectifier systems (see Fig. 11). The relatively low efficiency of the 6D6S system is mainly due to the high switching losses (see Fig. 9).

The input current of the active rectifier systems contains switching-frequency components which must be attenuated by a multistage EMC filter in order to ensure compliance to EMC standards. Besides differential-mode filtering there, special attention has to be paid to the common-mode filtering which prevents common-mode currents occurring due to the switching-frequency common-mode component of the rectifier output voltage and the parasitic capacitive coupling of the power semiconductors and the dc-side components to the heat sink and/or the safety ground. In contrast, for the 12-pulse system only a low-frequency common-mode output voltage component with three times the mains frequency is present which does not require special filtering.

For the 12-pulse system the dependency, of the output voltage on the load and mains condition has to be seen as a main drawback, besides the high system weight. For no-load operation the output voltage is determined by the amplitude of the line-to-line mains voltage, in the case at hand $U_{O,\max} = 323$ V (for $\hat{U}_N = 132$ V), and decreases to $U_{O,\min} = 233$ V (see Fig. 3) for rated load and maximum mains frequency $f_N = 800$ Hz. This voltage variation has to be accommodated in the design of the supplied PWM inverter and/or electric machine. For the active rectifier

TABLE III
MAIN POWER COMPONENTS EMPLOYED IN THE 5-kW BIDIRECTIONAL TWO-LEVEL PWM RECTIFIER SYSTEM

Part	Quantity	Type	Manufacturer	Typical Data	Package
L	3	196µH / 21.7Adc (33488)	Schott	Helical winding	168 Series
C	10	100µF / 250V / 105°C / YXF	Rubycon	1.2 A / 0.18 Ω	∅18 x 35.5 mm
D_F	6	15ETX06	IR	600 V / 15 A / 18 ns	TO220
D_S	6	20L15T	IR	15 V / 20 A	TO220
S	6	SPP20N60C3	Infineon	600 V/ 190mΩ	TO220

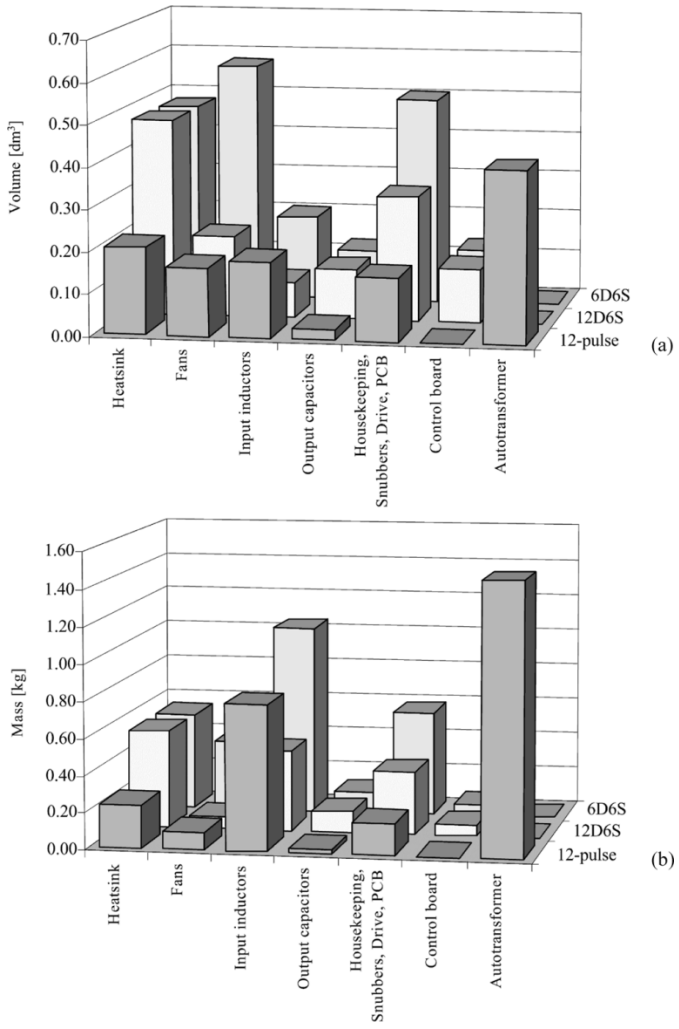

Fig. 10. Comparison of (a) volume and (b) weight of the main components of the rectifier concepts shown in Fig. 1 [12-pulse rectifier, cf. Fig. 1(a); 12D6S, cf. Fig. 1(b); and 6D6S, cf. Fig. 1(c)]; rated power: $P_O = 5$ kW.

systems an output voltage of $U_O = 350$ V is ensured independent of the load condition.

A further disadvantage could be the emission of acoustic noise dependent on the employed magnetic material and the mechanical construction of the input inductors and the autotransformer.

TABLE IV
TOTAL VOLUME, TOTAL WEIGHT, AND OVERALL SPECIFIC WEIGHT OF THE RECTIFIER CONCEPTS SHOWN IN FIG. 1. FOR ALL SYSTEMS A RATED POWER OF $P_O = 5$ kW HAS BEEN ASSUMED

System	Mass [kg]	Volume [dm³]	Specific weight [kg/dm³]
12-pulse rectifier	2.8	1.14	2.5
12D6S	1.6	1.3	1.2
6D6S	2.7	2.0	1.4

TABLE V
TYPICAL SPECIFIC WEIGHTS OF POWER COMPONENTS OF PWM RECTIFIER SYSTEMS

Component	Specific weight [kg/dm³]
Inductor (Schott 168 Series)	5.0
Electrolytic capacitor (450V)	3.0
Control board	1.2
Heatsink	1.2
Fan	0.7

In summary, the three-level rectifier system (12D6S) represents the most advantageous solution concerning volume, weight, and functionality as it allows for the supply of $1/\sqrt{3} \approx 58\%$ of the rated power at sinusoidal current also in case of a failure of a mains phase, i.e., for two-phase operation.

The weight of the 12-pulse system could be reduced by replacing the three individual magnetic cores of the autotransformer by a five-limb core. In connection with advantages of the system concerning complexity/reliability and robustness/overload capacity this motivates a further consideration of

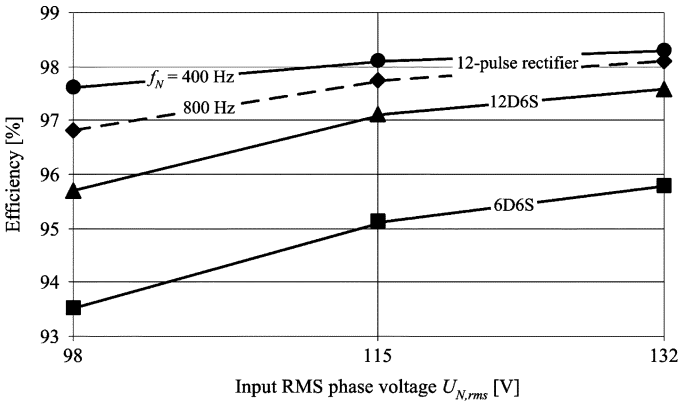

Fig. 11. Comparison of the power conversion efficiencies of the rectifier concepts shown in Fig. 1 (denomination as in Fig. 10) for different levels of the input voltage $U_{N,\mathrm{rms}} = 98$, 115, and 132 V; assumed operating frequency: $f_N = 400$ Hz; rated power: $P_O = 5$ kW.

the system. There, the main aim is an extension of the circuit topology to controlled output in order to eliminate the main drawback compared to active systems.

For the sake of completeness, a novel 12-pulse rectifier topology with controllable output voltage will be introduced and briefly discussed in the following in combination with results of a first experimental analysis. Concerning a more detailed analysis of the system we would like to refer to a future publication currently under preparation.

V. 12-Pulse Rectifier With Controlled Output Voltage

A controllability of the output voltage of a 12-pulse rectifier system [Fig. 1(a)] can be achieved by extending the basic topology as given in Fig. 12. There, the system shows the functionality of a boost converter. According to the duty cycle of the transistors T_1 and T_2 (which are preferably switched in an interleaved manner) the output voltage of the diode bridges and, therefore, the input voltage of the autotransformers is reduced. Accordingly, a higher dc voltage U_O is required for balancing the mains voltage. For guaranteeing a symmetric distribution of the mains current to the partial systems a zero-sequence current control has to be employed which is not discussed here for the sake of brevity.

First experimental results of the rectifier are shown in Fig. 12(b) and (c). With the exception of a ripple with switching frequency the shape of the mains current is identical to a passive 12-pulse rectifier. Also, in the shape of the input voltage of the autotransformer the typical 12-pulse waveform is obvious.

Furthermore, we want to point out that no sinusoidal PWM has to be performed and/or the transistors are controlled with essentially time-constant duty cycle which facilitates a very simple realization of the control and the transistor gate drive circuits. It is important to note that the output voltage control ensures a constant output voltage value but does not increase the power limit $P_{O,\max}$ of the system [see (9)].

VI. Conclusion

Passive rectifier systems for operation in the public mains, i.e., for a mains frequency of 50/60 Hz show a considerably higher volume than active rectifier systems of equal power.

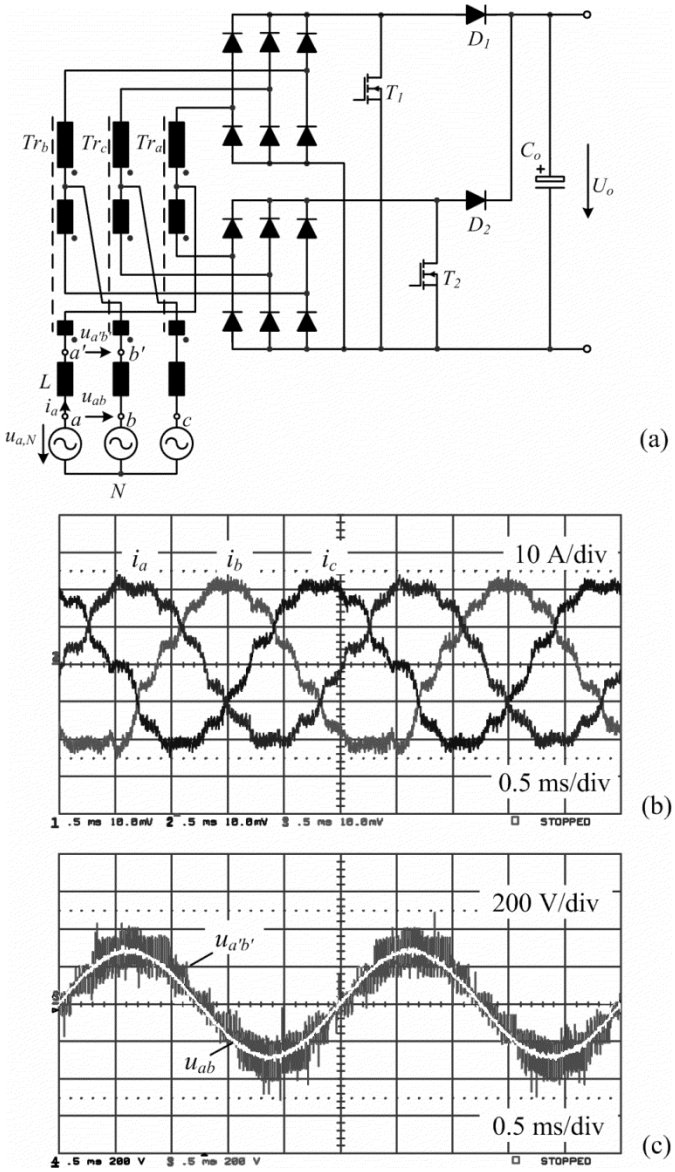

Fig. 12. (a) Experimental analysis of an extension of the passive 12-pulse rectifier system to controlled output voltage. The power transistors are operated in interleaved manner, the boost inductor is formed by the input inductors L and partly by the stray inductances of the interphase transformer. Furthermore shown: (b) time behavior of the mains phase currents. (c) Autotransformer input line-to-line voltage $u_{a'b'}$ and related mains line-to-line voltage u_{ab}. Operating parameters: $U_{N,\mathrm{rms}} = 115$ V; $f_N = 400$ Hz; $U_O = 350$ V; $P_O = 4.85$ kW; switching frequency $f_P = 33$ kHz; and efficiency $\eta = 95\%$.

However, as shown in this paper, an increase of the mains frequency by a factor of only 10 already results in an approximately equal power density $(\mathrm{W/dm^3})$ of both concepts. Therefore, the selection of the rectifier concept for supplying the PWM inverter stage of an EHA to be employed in future More Electric Aircraft can be based mainly on functionality and complexity/reliability.

Active rectifier systems are characterized by a controlled output voltage and a controlled sinusoidal shape of the input current and allow two-phase operation. However, one has to accept a relatively complex structure of the power and control circuits. The main aspects of a practical realization are, therefore, the integration of the power semiconductors into a multichip power module and a fully digital system control.

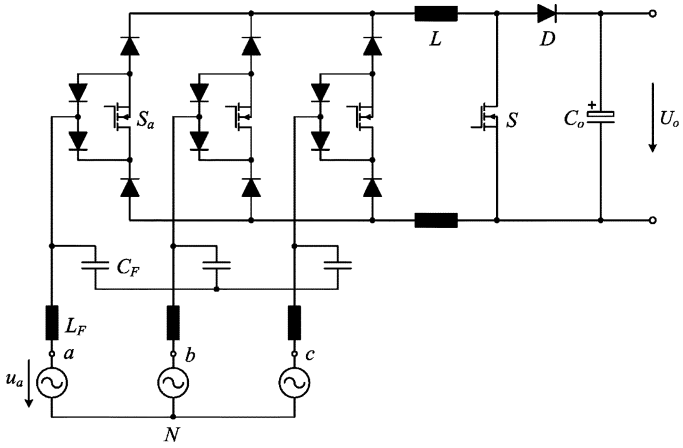

Fig. 13. Basic structure of the power circuit of a three-phase buck+boost PWM rectifier [15].

Considering the continuous progress in power semiconductor technology active systems shows the potential of a further increase of the power density with increasing switching frequency and/or decreasing volume of the passive components.

Passive 12-pulse rectifier systems are characterized by a low complexity/high reliability, even for an extension to controlled output voltage. As a first experimental analysis shows, the efficiency of a controlled 12-pulse system is comparable to a three-level active rectifier. However, asymmetries and harmonics of the mains voltage still influence the mains current quality. Also, the disadvantage of a high system weight will not be reduced significantly in the future due to lacking progress in the development of new magnetic materials.

In summary, the three-level PWM rectifier constitutes the most advantageous solution and should be considered as a reference for a comparison of further rectifier concepts. There, e.g., the performance of the three-phase buck + boost PWM rectifier topology [15] shown in Fig. 13 is of special interest as it allows a direct startup without output capacitor precharging and a direct limitation of the load current in case of an output short circuit and, therefore, ensures a high system reliability.

REFERENCES

[1] D. Van den Bossche, "More electric control surface actuation—a standard for the next generation of transport aircraft," in *Proc. Eur. Conf. Power Electronics and Applications*, 2003, CD-ROM.

[2] D. R. Trainer and C. R. Whitley, "Electric actuation—power quality management of aerospace flight control systems," in *Proc. IEE Int. Conf. Power Electronics, Machines and Drives*, 2003, pp. 229–234.

[3] A. M. Cross, A. J. Forsyth, D. R. Trainer, and N. Baydar, "Simulation of power quality issues in more electric aircraft actuator supplies," in *Proc. Eur. Conf. Power Electronics and Applications*, 2003, CD-ROM.

[4] J. W. Kolar and H. Ertl, "Status of techniques of three-phase rectifier systems with low effects on the mains," in *Proc. Int. Telecommunications Energy Conf.*, 1999, Paper 14-1.

[5] M. Depenbrock and C. Niermann, "A new 12-pulse rectifier circuit with line-side interphase transformer and nearly sinusoidal line currents," in *Proc. Int. Conf. Power Electronics and Motion Control*, 1990, pp. 374–378.

[6] J. W. Kolar and F. C. Zach, "A novel three-phase three-switch three-level PWM rectifier," in *Proc. Int. Conf. Power Conversion*, 1994, pp. 125–138.

[7] M. J. Provost, "The more electric aero-engine: a general overview from an engine manufacturer," in *Proc. IEE Int. Conf. Power Electronics, Machines and Drives*, 2003, pp. 246–251.

[8] P. W. Wheeler, L. Empringham, M. Apap, L. de Lilo, J. C. Clare, and K. Bradley, "A matrix converter motor drive for an aircraft actuation system," in *Proc. Eur. Conf. Power Electronics and Applications*, 2003, CD-ROM.

[9] J. Miniböck and J. W. Kolar, "Wide input voltage range high power density high efficiency 10 kW three-phase three-level unity power factor PWM rectifier," in *Proc. IEEE PESC'02*, 2002, pp. 1642–1648.

[10] S. Choi, P. N. Enjeti, and I. J. Pitel, "Polyphase transformer arrangements with reduced kVA capacities for harmonic current reduction in rectifier-type utility interface," *IEEE Trans. Power Electron.*, vol. 11, no. 5, pp. 680–690, Sep. 1996.

[11] G. Gong, U. Drofenik, and J. W. Kolar, "12-pulse rectifier for more electric aircraft applications," in *Proc. IEEE Int. Conf. Industrial Technology*, 2003, pp. 1096–1101.

[12] J. Miniböck, F. Stögerer, and J. W. Kolar, "A novel concept for mains voltage proportional input current shaping of a VIENNA rectifier eliminating controller multipliers. Part I—basic theoretical considerations and experimental verification," in *Proc. IEEE APEC'01*, 2001, pp. 582–586.

[13] J. W. Kolar, H. Ertl, and F. C. Zach, "Design and experimental investigation of a three-phase high power density high efficiency unity power factor PWM (VIENNA) rectifier employing a novel power semiconductor module," in *Proc. IEEE APEC'96*, 1996, pp. 514–523.

[14] ——, "Calculation of the passive and active component stresses of three-phase PWM converter systems with high pulse rate," in *Proc. Eur. Conf. Power Electronics and Applications*, 1989, pp. 1303–1311.

[15] M. Baumann and J. W. Kolar, "A novel control concept for reliable operation of a three-phase three-switch buck-type unity power factor rectifier with integrated boost output stage under heavily unbalanced mains condition," in *Proc. IEEE PESC'03*, 2003, pp. 3–10.

Guanghai Gong (S'03) was born in Zhejiang, China, in 1977. He received the B.Sc. and M.Sc. degrees in electrical engineering from Zhejiang University, Zhejiang, China, in 1999 and 2002, respectively. He is currently working toward the Ph.D. degree in the Power Electronic Systems Laboratory, Swiss Federal Institute of Technology (ETH) Zurich, Zurich, Switzerland.

His research interests include switched-mode power amplifiers, soft-switched dc/dc converters, and ac–dc converters for aircraft application.

Marcelo Lobo Heldwein (S'00) received the B.S. and M.S. degrees in electrical engineering from the Federal University of Santa Catarina, Florianópolis, Brazil, in 1997 and 1999, respectively. He is currently working toward the Ph.D. degree in the Power Electronic Systems Laboratory, Swiss Federal Institute of Technology (ETH) Zurich, Zurich, Switzerland.

Between 1999–2001, he was a Research Assistant at the Power Electronics Institute (INEP), Federal University of Santa Catarina. He was an Electrical Design Engineer with Emerson Energy Systems, Brazil and Sweden, from 2001 to 2003. His research interests include power-factor-correction techniques, static power converters, and electromagnetic compatibility.

Mr. Heldwein is a Member of the Brazilian Power Electronics Society (SOBRAEP).

Uwe Drofenik (S'96–M'00) was born in Moedling, Austria, in 1970. He received the M.Sc. and Ph.D. degrees in electrical engineering (both *cum laude*) from the University of Technology Vienna, Vienna, Austria, in 1995 and 1999, respectively.

He is currently performing scientific research and teaching at the Swiss Federal Institute of Technology (ETH) Zurich, Zurich, Switzerland, where he is developing web-based interactive educational software (www.ipes.ethz.ch). During 1996, he was a researcher at the Masada-Ohsaki Laboratory, The University of Tokyo, Japan. His research interests include thermal analysis of power systems, power-factor correction, single- and three-phase converters, numerical simulation, and Java programming. He authored 33 conference papers, five journal papers, and four patents.

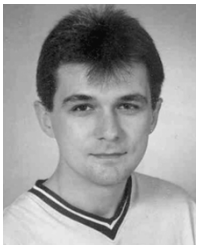

Johann Miniböck was born in Horn, Austria, in 1973. He received the Dipl.-Ing. (M.Sc.) degree in industrial electronics from the University of Technology Vienna, Vienna, Austria, in 1998. He is currently working toward the Ph.D. degree at the Swiss Federal Institute of Technology (ETH) Zurich, Zurich, Switzerland.

He is also teaching electrical machines, drives, and power electronics at a technical college and has recently started his own power electronics consulting company. He has performed various research projects in the field of single-phase and three-phase power-factor correction, switch-mode power supplies for various applications, and has developed a laboratory setup for teaching power electronics. He is the author or coauthor of 20 scientific papers and patents. His current research activities are focused on the hardware realization of a three-phase ac/ac sparse matrix converter and on driver circuits for high-power piezoelectric actuators.

Kazuaki Mino (S'04) was born in Tokyo, Japan, in 1968. He received the B.E. and M.E. degrees in electronics engineering from Tokyo Denki University, Tokyo, Japan in 1992 and 1994, respectively. He is currently working toward the Ph.D. degree in the Power Electronic Systems Laboratory, Swiss Federal Institute of Technology (ETH) Zurich, Zurich, Switzerland.

In 1994, he joined the Electronics Technology Laboratory at Fuji Electric Advanced Technology Company Ltd., Tokyo, Japan, where he has been working on the development of ac–ac converters (matrix converters, induction heating), power-factor-correction circuits, and dc-dc converters. His current research is focused on hybrid 12-pulse rectifiers and electronic inductors for high-power-density rectifiers.

Mr. Mino is a Member of the Institute of Electrical Engineers of Japan.

Johann W. Kolar (M'89–SM'04) studied industrial electronics at and received the Ph.D. degree (*summa cum laude*) from the University of Technology Vienna, Vienna, Austria.

From 1984 to 2001, he was with the University of Technology Vienna, where he was teaching and conducting research in close collaboration with industry in the fields of high-performance drives, high-frequency inverter systems for process technology, and uninterruptible power supplies. He has proposed numerous novel converter topologies, e.g., the VIENNA Rectifier system and the Three-Phase AC–AC Sparse Matrix Converter concept. He has authored more than 180 scientific papers published in international journals and conference proceedings and has filed over 50 patents. He was appointed Professor and Head of the Power Electronic Systems Laboratory at the Swiss Federal Institute of Technology (ETH) Zurich, Zurich Switzerland, in 2001. The focus of his current research is on novel ac–ac and ac–dc converter topologies with low effects on the mains for telecommunication systems, More-Electric-Aircraft applications, and distributed power systems utilizing fuel cells. A further main area of research is the realization of ultracompact intelligent converter modules employing the latest power semiconductor technology (SiC) and novel concepts for cooling and active EMC filtering.

Dr. Kolar is a Member of the Institute of Electrical Engineers of Japan and of Technical Program Committees of numerous international conferences in the field (e.g., Director of the Power Quality branch of the International Conference on Power Conversion and Intelligent Motion). From 1997 through 2000, he served as an Associate Editor of the IEEE TRANSACTIONS ON INDUSTRIAL ELECTRONICS and, since 2001, he has served as an Associate Editor of the IEEE TRANSACTIONS ON POWER ELECTRONICS.